Clathrates $Ba_8\{Zn,Cd\}_xSi_{46-x}$, x~7: synthesis, crystal structure and thermoelectric properties

2009 J. Phys.: Condens. Matter 21 385404

(http://iopscience.iop.org/0953-8984/21/38/385404)

J. Phys.: Condens. Matter **21** (2009) 385404 (8pp) doi:10.1088/0953-8984/21/38/385404

Clathrates $Ba_8\{Zn, Cd\}_xSi_{46-x}$, $x \sim 7$: synthesis, crystal structure and thermoelectric properties

N Nasir[1], A Grytsiv[1], N Melnychenko-Koblyuk[1], P Rogl[1,5], E Bauer[2], R Lackner[2], E Royanian[2], G Giester[3] and A Saccone[4]

[1] Institute of Physical Chemistry, University of Vienna, A-1090 Wien, Austria
[2] Institute of Solid State Physics, Vienna University of Technology, A-1040 Wien, Austria
[3] Institute of Mineralogy and Crystallography, University of Vienna, Althanstrasse 14, A-1090 Wien, Austria
[4] Dipartimento di Chimica e Chimica Industriale, Università di Genova, Via Dodecaneso 31, I-16146 Genova, Italy

E-mail: peter.franz.rogl@univie.ac.at

Received 23 February 2009
Published 27 August 2009
Online at stacks.iop.org/JPhysCM/21/385404

Abstract

Novel ternary type-I clathrate compounds $Ba_8\{Zn, Cd\}_xSi_{46-x}$, $x \sim 7$ have been synthesized from the elements by melting and reacting in quartz ampoules. Structural investigations for both compounds, i.e. x-ray single-crystal data at 300, 200 and 100 K for $Ba_8Zn_7Si_{39}$ and Rietveld data for $Ba_8Cd_7Si_{39}$, confirm cubic primitive symmetry consistent with the space group type $Pm\bar{3}n$ ($a_{Ba_8Zn_7Si_{39}} = 1.043\,72(1)$ nm; $a_{Ba_8Cd_7Si_{39}} = 1.058\,66(3)$ nm). Whereas for $Ba_8Zn_7Si_{39}$ site 16i is completely occupied by Si atoms, a random atom distribution with different Zn/Si ratio exists for the two sites, 6d (0.77Zn + 0.23Si) and 24k (0.91Si + 0.09Zn). No vacancies are encountered and all atom sites are fully occupied. This atom distribution is independent of temperature. Rietveld refinements for $Ba_8Cd_7Si_{39}$ show that the 6d site is fully occupied by Cd atoms, leaving only the 24k site for a random occupation (0.96Si + 0.04Cd) consistent with the chemical formula $Ba_8Cd_7Si_{39}$. The temperature-dependent x-ray spectra for $Ba_8Zn_7Si_{39}$ define an Einstein mode, $\Theta_{E,U33} = 80$ K. Studies of transport properties show electrons as the majority charge carriers in the system. Although the Cd- and Zn-based samples are isoelectronic, a significantly different electronic transport points towards substantial differences in the electronic density of states in both cases.

(Some figures in this article are in colour only in the electronic version)

1. Introduction

In recent studies of type-I clathrate systems $Ba_8M_xGe_{46-x}$ (M is a transition element, $x \sim 8$) we have dealt with the physical properties of Zn/Cd-containing clathrate germanide systems [1, 2] and have demonstrated that increasing Zn/Cd content drives the metallic system towards a metal-to-insulator transition. The present paper extends our systematic investigation to ternary clathrate phases in the homologous silicide systems, where compounds $Ba_8Zn_xSi_{46-x}$ and $Ba_8Cd_xSi_{46-x}$ are hitherto unknown.

[5] Author to whom any correspondence should be addressed.

A binary $Ba_8Ge_{43}\square_3$ (open squared box denotes vacancy) clathrate phase with three framework defects is stable only in the temperature range 770–810 °C [3, 4] while Ba–M–Si clathrates have no binary counterpart $Ba_8Si_{46-x}\square_x$ stable under normal pressure [5]. Superconducting hP-$Ba_{8-x}Si_{46}$ ($T_C = 9.0$ K, $x = 0.24$) is only stable above 3 GPa and at temperatures higher than 800 °C [6]. A simple Zintl count for $Ba_8\{Zn, Cd\}_8Si_{38}$, however, indicates proximity to semiconducting behaviour, which in turn may develop interesting thermoelectric properties. Therefore the main tasks of the present work are (a) to elucidate details of the crystal structure of novel ternary clathrates $Ba_8\{Zn, Cd\}_xSi_{46-x}$ and

(b) to investigate their physical properties (resistivity and thermopower). Furthermore two different routes of sample preparation, i.e. sintering powder compacts and hot-pressing, are employed.

2. Experimental details

Alloys with a weight of 2–4 g were prepared from elemental ingots (Ba 99.9, Zn, Cd 99.99 and Si 99.999 mass%) by reaction in vacuum-sealed quartz tubes at $T = 800\,^{\circ}\mathrm{C}$ for 4 days. Afterwards the reaction products were powdered to a particle size below 100 μm. Samples for physical property measurements were compacted in cylinders with diameter 10 mm and height 6 mm by (a) cold-pressing in a steel die (5 MPa) followed by sintering treatment (see below) and (b) hot-pressing in a graphite die at 800 °C (argon atmosphere, pressure 56 MPa, FCT hot-press system HP W 200/250 2200-200-KS). Cold- and hot-pressed cylindrical specimens were then annealed in vacuum-sealed quartz tubes at $T = 800\,^{\circ}\mathrm{C}$ for 2–4 days followed by quenching in cold water.

Single crystals of $Ba_8Zn_7Si_{39}$ were grown by a self-flux method from molten $Ba_8Zn_7Si_{39} + 10$Zn (mass%) that was cooled from 900 to 600 °C at a rate of 3 °C h^{-1}. The metal flux was dissolved in hydrochloric acid. Inspection on an AXS-GADDS texture goniometer ensured high crystal quality, unit cell dimensions and Laue symmetry of the specimens prior to x-ray intensity data collection on a four-circle Nonius Kappa diffractometer equipped with a CCD area detector employing graphite monochromated Mo Kα. No absorption correction was necessary because of the rather regular crystal shape and small dimensions of the investigated specimen. Orientation matrix and unit cell parameters for a cubic system were derived using the program DENZO. The structure was solved by direct methods and refined with the SHELXL-97 and SHELXS-97 programs. X-ray powder diffraction (XPD) data were collected with a Guinier–Huber image plate system (Cu Kα_1 or Fe Kα_1; $8^{\circ} < 2\theta < 100^{\circ}$). Precise lattice parameters were calculated by least-squares fits to indexed 2θ values employing Ge as an internal standard ($a_{\mathrm{Ge}} = 0.565\,791$ nm). The x-ray powder diffraction intensity spectra were analysed by Rietveld refinements [7].

The hot-pressed samples were polished using standard procedures and were examined by optical metallography and scanning electron microscopy (SEM). Compositions for hot-pressed samples were determined via electron probe micro-analyses (EPMA) on a Carl Zeiss EVO 40 equipped with a Pentafet Link EDX system operated at 20 kV. Physical properties, which comprise electronic and thermal transport as well as thermoelectricity (details are given in [1, 2]), were measured on both sintered and hot-pressed samples of Zn-containing clathrates and on hot-pressed samples of Cd-containing clathrate (due to a lack of dense sintered samples for Cd clathrates).

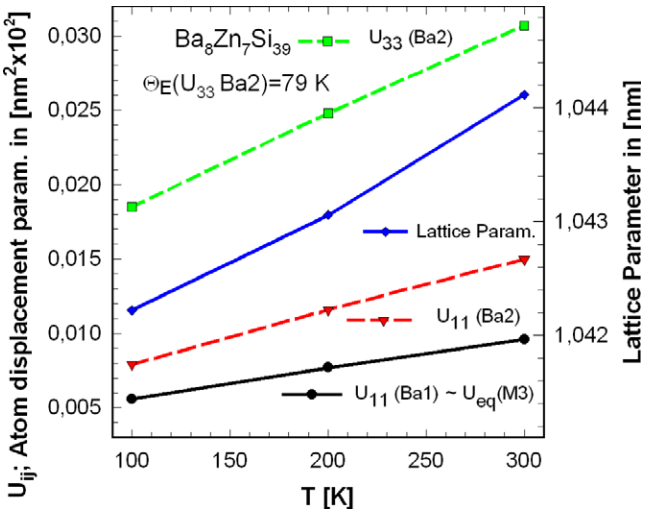

Figure 1. Temperature displacement parameters and lattice parameters of $Ba_8Zn_7Si_{39}$ versus temperature.

3. Results and discussion

3.1. Crystal structures of $Ba_8Zn_7Si_{39}$ and $Ba_8Cd_7Si_{39}$

For a single crystal, grown by the self-flux method from molten $Ba_8Zn_7Si_{39} + 10$Zn (mass%), x-ray intensity data were collected at three temperatures, 100, 200 and 300 K, in order to evaluate atom site preferences. Extinctions were consistent with a primitive cubic lattice (space group $Pm\bar{3}n$, ($a = 1.043\,72(1)$ nm)) and indicated isotypism with the structure of clathrate type-I for all temperatures studied. No extra reflections were detected that would indicate a larger unit cell $a' = 2a$ as reported for binary $Ba_8Ge_{43}\square_3$ [4]. The heavy barium atoms were unambiguously found in sites 2a (0, 0, 0) and 6c (1/4, 0, 1/2). With a significant difference in the x-ray scattering power of Zn and Si atoms, the electron density distribution for the remaining sites appeared as follows (at 300 K): (i) Wyckoff site 16i is completely occupied by Si atoms, whereas (ii) a random atom distribution with a different Zn/Si ratio is found for the two sites 6d ($0.77\mathrm{Zn} + 0.23\mathrm{Si}$) and 24k ($0.91\mathrm{Si} + 0.09\mathrm{Zn}$). There is practically no change in atom distribution as a function of temperature. From the relative size of the rather isotropic atom displacement parameters for the sites 6d, 16i and 24k, vacancies seem not to play a significant role and all sites are found to be fully occupied. The structure refinement yields an overall formula $Ba_8Zn_7Si_{39}$ close to the nominal starting composition and to EPMA (in at.% $Ba_{15.3}Zn_{13.4}Si_{71.3} = Ba_8Zn_{7.0}Si_{37.3}$). Table 1 summarizes all crystallographic information derived from the structure determination. Interatomic distances are consistent with the sum of atomic radii.

The ADP parameters for Ba atoms located in the 6c site (Ba2) show a significant anisotropy in contrast to Ba1 atoms, which seem to have normal behaviour (table 1 and figure 1). Similarly ADP's of framework atoms reveal a rather spherical atom shape, also indicative of the absence of any significant amount of vacancies in the framework. If the $Ba_8Zn_7Si_{39}$ crystal is considered as a simple Debye solid with

Table 1. X-ray single-crystal data for $Ba_8Zn_7Si_{39}$ at various temperatures (ω scans, scan width 2°; redundancy > 12) and x-ray powder diffraction (XPD) data for $Ba_8Cd_7Si_{39}$; both compounds isotypic with clathrate type-I; space group $Pm\bar{3}n$; no. 223; structure settings standardized with program *Structure Tidy* [14].

Parameter/temperature	SC, 300 K	SC, 200 K	SC, 100 K	XPD, 300 K
Formula from refinement	$Ba_8Zn_{6.9}Si_{39.1}$	$Ba_8Zn_{7.0}Si_{39.0}$	$Ba_8Zn_{6.9}Si_{39.1}$	$Ba_8Cd_{6.8}Si_{39.2}$
Crystal size	80 × 54 × 70	80 × 54 × 70	80 × 54 × 70	—
a (nm)	1.044 12(2)	1.043 06(2)	1.042 22(2)	1.058 66(3)
μ_{abs} (mm^{-1})	11.38	11.40	11.43	
Data collection,				
2Θ range (deg)	$2 \leqslant 2\Theta \leqslant 72.6$; 130 s/frame	$2 \leqslant 2\Theta \leqslant 72.0$; 130 s/frame	$2 \leqslant 2\Theta \leqslant 72.5$; 130 s/frame	$8 \leqslant 2\Theta \leqslant 100$
Total number of frames	188; 6 sets	188; 6 sets	188; 6 sets	
Reflections in refinement	$421 \geqslant 4\sigma(F_o)$ of 527 [1836]	$422 \geqslant 4\sigma(F_o)$ of 519 [1805]	$436 \geqslant 4\sigma(F_o)$ of 21 [1811]	141
Number of variables	20	20	20	18
Mosaicity	<0.45	<0.46	<0.44	$R_F = \Sigma\|F_o - F_c\|/\Sigma F_o = 0.055$
$R_F^2 = \Sigma\|F_o^2 - F_c^2\|/\Sigma F_o^2$	0.0175	0.0160	0.0160	$R_I = \Sigma\|I_o - I_c\|/\Sigma I_o = 0.074$
R_{Int}	0.066	0.066	0.067	$R_{wP} = [\Sigma w_i\|y_{oi} - y_{ci}\|^2/\Sigma w_i\|y_{oi}\|^2]^{1/2} = 0.063$
wR2	0.039	0.036	0.037	$R_P = \Sigma\|y_{oi} - y_{ci}\|/\Sigma\|y_{oi}\| = 0.045$
GOF	1.098	1.113	1.152	$R_e = [(N - P + C)/\Sigma w_i y_{oi}^2]^{1/2} = 0.017$
Extinction (Zachariasen)	0.0028(2)	0.0014(1)	0.0010(1)	$\chi^2 = (R_{wP}/R_e)^2 = 14.2$
Ba1 in 2a (0, 0, 0); occ.	1.00(1)	1.00(1)	1.00(1)	1.015(5)
$U_{11} = U_{22} = U_{33}$	0.009 59(9)	0.0077(1)	0.005 60(9)	B_{iso} (in 10^2 nm^2) = 0.45(4)
Ba2 in 6c (1/4, 0, 1/2); occ.	1.00(—)	1.00(—)	1.00(—)	1.02(3)
U_{11}; $U_{22} = U_{33}$	0.0150(1); 0.0307(1)	0.0116(1); 0.0248(1)	0.0079(1); 0.0185(1)	B_{iso} (in10^2 nm^2) = 1.38(5)
M1 in 6d (1/4, 1/2, 0); occ.	0.226(3) Si + 0.774Zn	0.226(3) Si + 0.774Zn	0.228(3) Si + 0.772Zn	1.01(1)Cd
U_{11}; $U_{22} = U_{33}$	0.0106(2); 0.0089(2)	0.0082(2); 0.0066(2)	0.0052(2); 0.0043(2)	B_{iso} (in 10^2 nm^2) = 1.08
SI2 in 16i (x, x, x); occ.	1.008(3)	1.007(3)	1.012(4)	1.02(3)
x	0.184 62(4)	0.184 63(3)	0.184 59(4)	0.1835(2)
$U_{11} = U_{22} = U_{33}$; $U_{23} = U_{13} = U_{12}$	0.0083(1); −0.0008(1)	0.0066(1); −0.0007(1)	0.0048(1); −0.0004(1)	B_{iso} (in 10^2 nm^2) = 0.95(8)

Table 1. (Continued.)

Parameter/temperature	SC, 300 K	SC, 200 K	SC, 100 K	XPD, 300 K
M3 in 24k (0, y, z); occ.	0.907(2) Si + 0.093Zn	0.905(2) Si + 0.095Zn	0.907(1) Si + 0.093Zn	0.96(1) Si + 0.04Cd
y; z	0.117 87(5); 0.305 24(5)	0.117 85(4); 0.305 30(4)	0.117 84(5). 0.305 37(5)	0.1151(2); 0.2968(3)
U_{11}; U_{22}; U_{33}	0.0096(2); 0.0101(2)	0.0075(2); 0.0078(2)	0.0052(2); 0.0059(2)	B_{iso} (in 10^2 nm^2) = 1.15(7)
U_{23} (in 10^2 nm^2)	0.0092(2); 0.0001(1)	0.0076(2); 0.0001(1)	0.0058(2); 0.0002(1)	
Residual density; max; min	0.82; −1.11	1.01; −1.04	0.67; −1.11	
Principal mean square atomic displacements U	Ba1 0.0096 0.0096 0.0096 Ba2 0.0307 0.0307 0.0151 M1 0.0106 0.0089 0.0089 Si2 0.0092 0.0092 0.0067 M3 0.0101 0.0096 0.0092	Ba1 0.0077 0.0077 0.0077 Ba2 0.0248 0.0248 0.0116 M1 0.0082 0.0066 0.0066 Si2 0.0073 0.0073 0.0053 M3 0.0079 0.0076 0.0075	Ba1 0.0056 0.0056 0.0056 Ba2 0.0185 0.0185 0.0079 M1 0.0052 0.0044 0.0044 Si2 0.0053 0.0053 0.0039 M3 0.0062 0.0055 0.0055	
Interatomic distances, standard deviation less than 0.0002 nm				
Ba1–8Si2	0.3339	0.3335	0.3332	0.3365
12M3	0.3416	0.3413	0.3411	0.3370
Ba2–8M3	0.3530	0.3526	0.3523	0.3622
4M1	0.3691	0.3688	0.3685	0.3743
8Si2	0.3876	0.3872	0.3869	0.3936
4M3	0.4031	0.4027	0.4025	0.4105
M1–4M3	0.2457	0.2454	0.2452	0.2582
4Ba2	0.3691	0.3688	0.3685	0.3743
Si2–1Si2	0.2365	0.2362	0.2361	0.2395
3M3	0.2406	0.2404	0.2402	0.2439
1Ba1	0.3339	0.3335	0.3332	0.3365
M3–2Si2	0.2406	0.2404	0.2402	0.2395
1M1	0.2457	0.2454	0.2452	0.2437
1M3	0.2461	0.2459	0.2456	0.2582
1Ba1	0.3416	0.3413	0.3411	0.3370
2Ba2	0.3530	0.3526	0.3523	0.3622

Ba2 atoms behaving like Einstein oscillators, the thermal displacements and the Einstein temperatures $\Theta_{E,ii}$ are related by

$$U_{ii} = \frac{\hbar^2}{2m_{Ba}k_B\Theta_{E,ii}} \coth\left(\frac{\Theta_{E,ii}}{2T}\right),$$

where m_{Ba} is the atomic mass of Ba. From the linear slope $\Delta U_{ii}/\Delta T$ in figure 1 the force constants, $K_{ii} = 4\pi^2 m \nu_{ii}$, Ba^2 (g s^{-2}), the frequency of vibrations ν_{ii} (10^{12} s^{-1}) and hence the Einstein temperatures $\Theta_{E,ii}$ (K) can be extracted. From symmetry constraints U_{11} is different from $U_{22} = U_{33}$ yielding $\Theta_{E,11} = 99$ K and $\Theta_{E,33} = 80$ K in line with a slightly flattened rotational ellipsoid of Ba2 atoms. Although from symmetry constraints U_{11} is different from $U_{22} = U_{33}$ the linear slopes $\Delta U_{ii}/\Delta T$ are indifferent for ADP parameters of framework atoms. A contour plot of electron density for the Ba2 atom at 100 K from a difference Fourier synthesis $F_{obs-Ba2}$, as shown in figure 2, revealed a rather uniform and round shape with little hints towards off-centre positions of the Ba2 atom. Off-centre behaviour was recently documented from low temperature neutron diffraction on a single crystal of $Ba_8Zn_8Ge_{38}$ [8]. It is interesting to note that Ba1 atoms (spherical by symmetry) do not show a thermal displacement factor enhanced over the general ADP values for framework atoms. Thus no special rattling or off-centre effect can be observed for Ba1 atoms. Rietveld refinement of the x-ray powder data for the alloy with nominal composition $Ba_8Zn_8Si_{38}$ is in perfect agreement with the observed intensities and with the atomic parameters derived from the single-crystal study and again yields a formula $Ba_8Zn_7Si_{39}$.

Due to a lack of single crystals for the Cd-containing specimen, the x-ray powder intensity spectrum for nominal composition $Ba_8Cd_8Si_{38}$ was analysed. Indexing prompted a cubic unit cell close to that established for $Ba_8Zn_7Si_{39}$. Analysis of the x-ray intensities, absence of systematic extinctions and size of the unit cell suggest isotypism with the structure type of clathrate I. Results of Rietveld refinements are compiled in table 1. Comparing the structural details for the two novel compounds $Ba_8\{Zn, Cd\}_7Si_{39}$ we observe that the 6d site (M1) is fully occupied by Cd atoms, and unambiguously reveals a random occupation of 0.96Si + 0.04Cd for the 24k site (M3), resulting in the chemical formula $Ba_8Cd_{6.8}Si_{39.2}$, in good agreement with EPMA data that yield 6.1 Cd per unit cell.

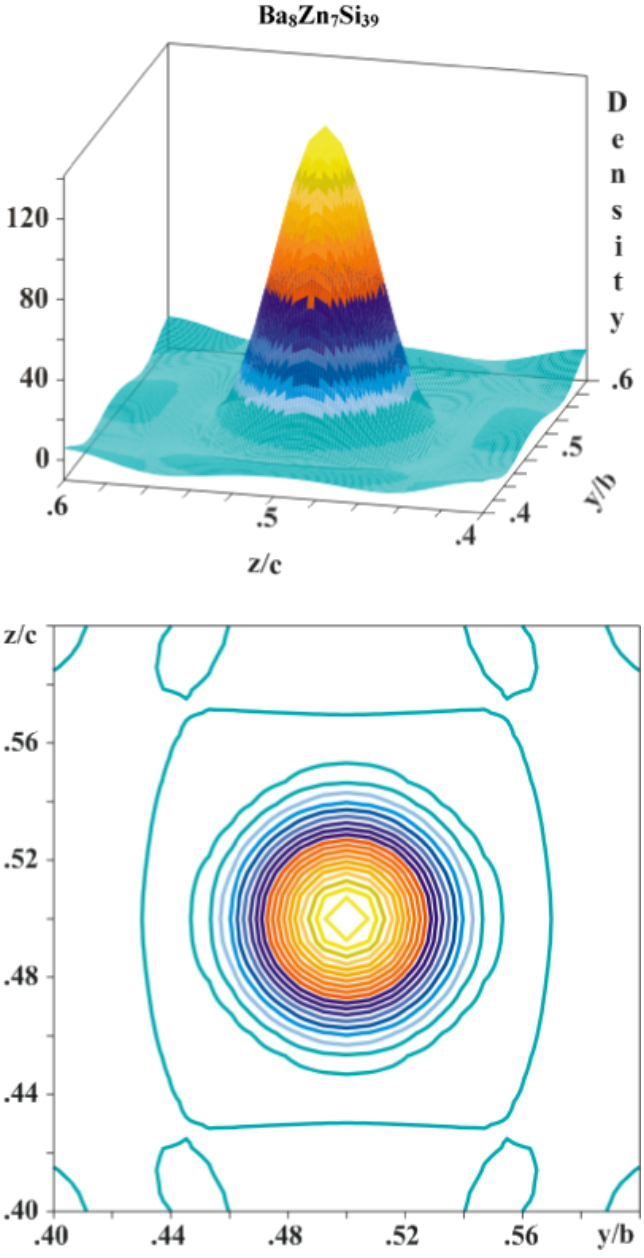

Figure 2. Contour plot of electron density at 100 K for Ba2 atom from difference Fourier $F_{obs-Ba2}$ (top: three-dimensional view, bottom projection on y–z plane)

3.2. Homogeneity regions of clathrates $Ba_8\{Zn, Cd\}_xSi_{46-x}$

XPD and EPMA of samples, prepared for $x = 3$, 6, 8, 8.5, 9 and 10 and annealed at 800 °C consistently yielded lattice parameters with only a small scatter ($a = 1.043\,69(2)$–$1.044\,12(2)$ for the Zn clathrate and $a = 1.058\,17(2)$ to $1.058\,66(2)$ for the Cd clathrate), indicating a homogeneity region of not more than ∼1 at.% (Zn or Cd) consistent with EPMA data, which for all alloys revealed a chemical formula of $Ba_8Zn_{6.9}Si_{39.1}$ and $Ba_8Cd_{6.1}Si_{39.9}$, respectively. As the error bar on the EDAX–EPMA data is about 1 at.% Zn but about 1.8 at.% Cd we assume for both compounds the formula $Ba_8\{Zn, Cd\}_{\sim 7}Si_{\sim 39}$, referring to our detailed structural analyses (see above). With the composition defined, samples for physical property measurements were prepared (see section 2). The single-phase condition could be attained from a nominal starting composition $Ba_8\{Zn, Cd\}_8Si_{38}$ with about an extra 2% Zn(Cd) to compensate for evaporation of the metals during preparation. The final product contained less than 2% secondary phases such as Si + $Ba\{Zn, Cd\}_2Si_2$.

Whereas the germanium-based clathrate systems $Ba_8\{Zn, Cd\}_xGe_{46-x}$ reveal a continuous solid solution deriving from binary $Ba_8Ge_{43}\square_3$ [1, 2], $Ba_8\{Zn, Cd\}_7Si_{39}$ clathrates have no binary counterpart $Ba_8Si_{46-x}\square_x$ ($Ba_8Si_{46-x}\square_x$ is not stable at 800 °C under normal pressure [5, 6]) and consequently exhibit only a very small homogeneity range in the ternary. In both

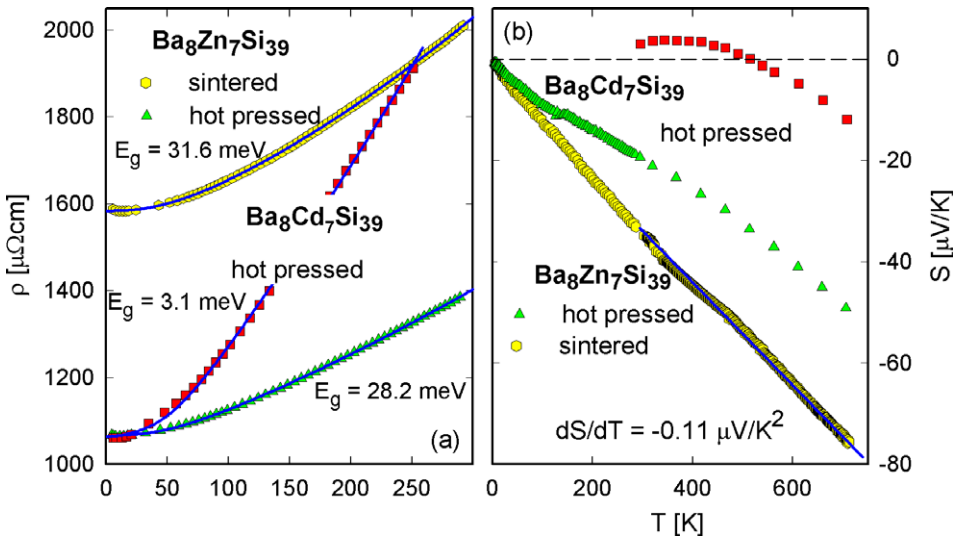

Figure 3. (a) Temperature-dependent resistivity ρ of $Ba_8Zn_7Si_{39}$. The solid line is a least-squares fit according to the model described in the text. (b) Temperature-dependent thermopower for $Ba_8Zn_7Si_{39}$ and $Ba_8Cd_7Si_{39}$. The solid line reveals $dS/dT = -0.11\ \mu V\ K^{-1}$.

cases, however, Zn, Cd metals can be considered as stabilizers of a truly ternary type-I clathrate silicide compound.

3.3. Transport properties

To characterize $Ba_8Zn_7Si_{38}$ and $Ba_8Cd_7Si_{38}$, measurements of electrical resistivity, thermal conductivity and thermopower were performed from 4 K to room temperature. A comparison of the physical property data for sintered and hot-pressed samples (see figures 3(a) and (b)) clearly identified the hot-pressed samples as the lower resistance materials ($\rho_0 \sim 1050\ \mu\Omega$ cm for both the Zn and the Cd compound). While, however, there are no significant differences in the temperature-dependent resistivities of both Zn-based compounds, $\rho(T)$ of $Ba_8Cd_7Si_{39}$ exhibits a much steeper slope as a consequence of an almost doubled electron–phonon interaction constant. This parameter enters the Bloch–Grüneisen equation, determining $d\rho/dT$ of a simple metal.

A closer inspection of the resistivity data of both compounds shows, however, that $\rho(T)$ in figure 3(a) does not resemble simple metals due to a slightly positive curvature in the temperature range studied. However, adopting a model, which combines the description of simple metals via the Bloch–Grüneisen law with a temperature-dependent charge carrier density, yields an acceptable fit. The most relevant assumptions in this model are an electronic density of state (DOS) represented by a rectangular band where the Fermi energy is located below the band edge, followed by a gap E_g. The charge carrier density is then calculated via standard statistics considering the Fermi–Dirac distribution function [1, 9]. At $T = 0$, the narrow band of unoccupied states above E_F ensures a metallic behaviour. Once this region of the DOS becomes occupied by scattered conduction electrons, further electrons have to be promoted across the gap.

Least-squares fits yield good agreement with the experimental data (solid lines, figure 3(a)) when taking the gap widths $E_g = 3.1$ meV as the principal parameter for the Cd-based compound. The similarity of E_g in the case of both $Ba_8Zn_7Si_{39}$ samples ($E_g = 28.2$ and 31.6 meV) shows that the sintered and the hot-pressed specimens do not differ very much in their electronic structures. The Cd-based compound, in fact, appears to be different, although both Zn and Cd are isoelectronic elements. This difference is reflected in the temperature-dependent thermopower S of both compounds, plotted in figure 3(b). The almost linear temperature dependence of $S(T)$ for $Ba_8Zn_7Si_{39}$ suggests a simple origin, depending primarily on the charge carrier density n.

As already shown by Blatt [10] in terms of a free electron model, the diffusion thermopower can be expressed as

$$S_d(T > \Theta_D) = \frac{\pi^2 k_B^2 2m}{e\hbar^2 (3n\pi^2)^{\frac{2}{3}}} T \qquad (1)$$

where m is the mass of the charge carriers and e is the carrier charge. Equation (1) is valid for $T > \Theta_D$. For low temperatures ($T \ll \Theta_D$), where scattering on impurities dominates, S_d ($T \ll \Theta_D$) $= 1/3$ ($S_d(T > \Theta_D)$). Approaching the data of figure 3(b) by a linear dependence yields the charge carrier density $n_S = 2.5 \times 10^{21}$ cm^{-3} (referring to electrons as the principal charge carriers and $m = m_e$). In order to disentangle the influences of m and n on S_d, we have independently determined the charge carrier density n via room temperature Hall measurements arriving at $n = 6 \times 10^{20}$ cm^{-3}. Equation (1) would then imply an effective mass of $m = 0.4m_e$, well in agreement with similar data reported by [11] for clathrate $Sr_8Ga_{16}Ge_{30}$. The hot-pressed sample $Ba_8Zn_7Si_{39}$ shows a similar temperature dependence as the sintered one, although $|dS/dT|$ is smaller. As inferred already from resistivity measurements, the thermopower deduced for $Ba_8Cd_7Si_{39}$ behaves qualitatively different from the homologous Zn-based clathrates pointing to different features of the DOS at E_F: whereas at low temperatures small and positive values of $S(T)$ are deduced, thermopower changes

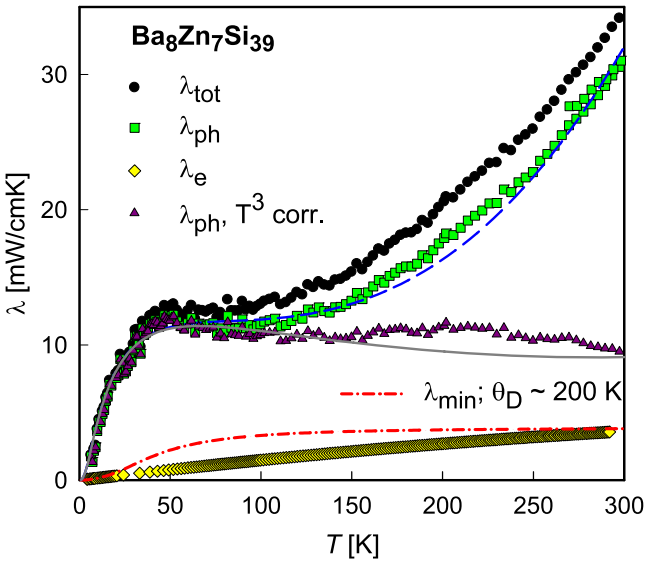

Figure 4. Temperature-dependent thermal conductivity λ (filled circles) of hot-pressed $Ba_8Zn_7Si_{39}$. The electronic contribution λ_e is displayed as filled diamonds and the lattice thermal conductivity $\lambda_{ph} = \lambda - \lambda_e$ is shown as filled squares. The dashed line is a least-squares fit according to equation (1), including a T^3 term correction for heat losses. The solid line represents the phonon term reduced by the T^3 term. The dashed–dotted line is the minimum thermal conductivity according to the model of Cahill and Pohl [12].

sign around 510 K to become negative. For simple materials, such behaviour would indicate a change of the principal charge carrier type from holes ($T < 500$ K) to electrons for $T > 500$ K.

The temperature-dependent thermal conductivity, λ, of $Ba_8Zn_7Si_{39}$ is shown in figure 4. The overall $\lambda(T)$ values are rather small, expected for cage-forming compounds, which are filled by loosely bound electropositive elements. Comparing the measured $\lambda(T)$ data with those of homologous $Ba_8Zn_{7.7}Ge_{38.3}$ [2] shows the lack of a pronounced low temperature maximum. The large initial rise of $\lambda(T)$ found for $Ba_8Zn_{7.7}Ge_{38.3}$ [2] results from much weaker boundary and point defect scattering in comparison to $Ba_8Zn_7Si_{39}$. A quantitative description of $\lambda(T)$ is possible in terms of Callaway's theory [13] of lattice thermal conductivity, λ_{ph}. To derive λ_{ph} from the total thermal conductivity λ, the Wiedemann–Franz law is applied to the $\rho(T)$ data, yielding the electronic thermal conductivity, λ_e. Although this model is valid in extended temperature ranges only for free electron systems, it is widely used even for complex materials such as skutterudites or clathrates. The Wiedemann–Franz relation states that increasing electrical resistivities cause decreasing λ_e values. Thus, the large overall resistivity of the present sample is the cause that λ_e is clearly the minority channel of the total measured effect and does not exceed 3.5 mW cm^{-1} K^{-1} at $T = 300$ K (see figure 4).

The temperature dependence of λ_{ph} follows from the basic thermodynamic expression $\lambda = (1/3)C_V v l$, where C_V is the heat capacity of the system, v the particle velocity and l the mean free path. According to Callaway [11], this transforms for the heat carrying lattice vibrations to

$$\lambda_{ph} = \frac{k_B}{2\pi^2 \upsilon_s}\left(\frac{k_B}{\hbar}\right)^3 T^3 \int_0^{\theta_D/T} \frac{\tau_c x^4 e^x}{(e^x-1)^2}\,dx$$
$$\upsilon_s = \frac{k_B \theta_D}{\hbar(6\pi^2 N)^{1/3}} \quad \text{and} \quad x = \frac{\hbar\omega}{k_B T} \tag{2}$$

with υ_s the velocity of sound, N the number of atoms per unit volume and ω the phonon frequency. τ_c^{-1} is the sum of the reciprocal relaxation times consisting of point defect scattering τ_D^{-1}, umklapp processes τ_U^{-1}, boundary scattering τ_B^{-1} and scattering of phonons by electrons τ_E^{-1}, i.e.

$$\tau_c^{-1} = \tau_B^{-1} + \tau_D^{-1} + \tau_U^{-1} + \tau_E^{-1}. \tag{3}$$

Equation (3) does not contain terms for resonance scattering, since they seem to be of minor importance for $Ba_8Zn_7Si_{39}$. A least-squares fit of equation (3) to the experimental data is shown in figure 4 as a solid line, revealing reasonable agreement for a Debye temperature $\Theta_D = 200$ K. In order to get rid of radiation losses, proprietary to the steady state heat flow method used, a T^3 term was added to equation (2). The fact that only a weak local maximum is observed around 50 K refers to distinct influences of phonon scattering on grain boundaries and point defects, in accordance with the large electrical resistivity observed. An approximation according to Cahill and Pohl [12], defines a lower theoretical limit of the lattice thermal conductivity, which primarily depends on the number of atoms per unit volume and on the Debye temperature. Taking $N = 4.74 \times 10^{28}$ m^{-3} and $\Theta_D = 200$ K reveals $\lambda_{min}(300\text{ K}) \sim 4$ mW cm^{-1} K^{-1}.

4. Conclusion

Novel type-I clathrates $Ba_8\{Zn, Cd\}_{\sim 7}Si_{\sim 39}$ have been found to exist at 800 °C with no appreciable homogeneity range. Single-crystal data for $Ba_8Zn_7Si_{39}$ show a random Zn/Si atom distribution in atom sites 6d and 24k. The 6d site is completely occupied by Cd atoms. Electronic transport for both compounds is metallic-like and electrons are the majority charge carriers in $Ba_8Zn_7Si_{39}$. While holes are the principal charge carriers for $Ba_8Cd_7Si_{39}$ at low temperatures, the type of conductivity changes for temperatures above ∼500 K. The rather large charge carrier density, $n = 6 \times 10^{20}$ cm^{-3} for $Ba_8Zn_7Si_{39}$, may explain the moderate Seebeck coefficient observed and the low figure of merit $ZT_{500\text{ K}} < 0.04$. The relatively low thermal conductivity for light framework clathrates (Si-based) may originate in part from a distinct rattling mode of Ba(2) atoms with an Einstein temperature of about 80 K as derived from the temperature-dependent Debye–Waller factor. It is interesting to note that the electron density for the Ba(2) atoms offers little evidence for an off-centre atom position.

Acknowledgments

The research reported herein was supported by the Higher Education Commission of Pakistan (HEC) under the scholarship

scheme 'PhD in Natural and Basic Sciences from Austria', by the FFG project 'THEKLA' and the Austrian FWF projects P19165 and P16778-No2.

References

[1] Melnychenko-Koblyuk N, Grytsiv A, Berger St, Kaldarar H, Michor H, Röhrbacher F, Royanian E, Bauer E, Rogl P, Schmid H and Giester G 2007 *J. Phys.: Condens. Matter* **19** 046203

[2] Melnychenko-Koblyuk N, Grytsiv A, Berger St, Kaldarar H, Michor H, Röhrbacher F, Royanian E, Bauer E, Rogl P, Schmid H and Giester G 2007 *J. Phys.: Condens. Matter* **19** 216223

[3] Carrillo-Cabrera W, Curda J, Petters K, Baenitz M, Grin Y and von Schnering H G 2000 *Z. Kristallogr. New Cryst. Struct.* **215** 321

[4] Carrillo-Cabrera W, Budnyk S, Prots Y and Grin Y 2004 *Z. Anorg. Allg. Chem.* **630** 2267

[5] Pauling File Binaries Edition, release 2002/1 Version 1.0, ASM Intl, Materials Park, OH, USA

[6] Fukuoka H, Kiyoto J and Yamanaka S 2004 *J. Phys. Chem. Solids* **65** 333–6

[7] Roisnel T and Rodriguez-Carvajal J 2001 *Mater. Sci. Forum* **118** 378–81

[8] Christensen M and Iversen B B 2008 *J. Phys.: Condens. Matter* **20** 104244

[9] Berger St 2003 *PhD Thesis* Vienna University of Technology Vienna, Austria

[10] Blatt F J 1968 *Physics of Electronic Conduction in Solids* (*McGraw-Hill Series in Materials Science and Engineering*) (New York: McGraw-Hill)

[11] Nolas G, Cohn J L, Slack G A and Schuman S B 1998 *Appl. Phys. Lett.* **73** 178

[12] Cahill D and Pohl R 1989 *Solid State Commun.* **70** 927

[13] Callaway J and von Baeyer H C 1960 *Phys. Rev.* **120** 1149

[14] Parthé E, Gelato L, Chabot B, Penzo M, Cenzual K and Gladyshevskii R 1994 *TYPIX-Standardized Data and Crystal Chemical Characterization of Inorganic Structure Types* (Berlin: Springer)